Position dependent surface quality in selective laser melting

Hitzler, L., Hirsch, J., Merkel, M., Hall, W., Öchsner, A., 2017. Position dependent surface quality in Selective Laser Melting. Mat.-wiss. u. Werkstofftech. 48, 327-334.

http://dx.doi.org/10.1002/mawe.201600742.

Position dependent surface quality in selective laser melting

Positionsabhängige Oberflächenqualität im selektiven Laserstrahlschmelzen

L. Hitzler [a], J. Hirsch [b], M. Merkel [b], W. Hall [a], A. Öchsner [a]

[a] Griffith School of Engineering, Griffith University, Gold Coast Campus, Southport 4222, Australia
[b] Aalen University of Applied Sciences, 73430 Aalen, Germany

Additive manufacturing receives nowadays opulent attention in both media and ongoing research. In particular, the techniques involving full melting of the raw material, enabling the fabrication of directly deployable components, are of high interest. To date, there are still secondary influences which are yet to be considered, leading to substantial, mainly directional dependent, deviations. The study at hand investigated the surface roughness dependencies in plane, focusing on the interaction of the unidirectional inert gas stream with the irradiation sequence; more precisely the weld splashes emerging from the melt pool, and the resulting in plane pattern. The surface roughness of the upwards orientated faces revealed clear fluctuations, being lowest close to the gas-inlet and also in the back area of the machine. Perpendicular to the fabrication plane aligned surfaces did not reveal any volatility regarding the inert gas stream. Increasing the energy density of the irradiation led to an increase in the surface roughness of all side faces, but to an improved roughness of the upwards facing surfaces coupled with a significant reduction in evident weld splashes.

Corresponding author: Leonhard Hitzler, Griffith University, Southport, QLD, 4222
E-Mail: Leonhard.Hitzler@Griffithuni.edu.au

Keywords: Powder-bed based Additive Manufacturing, Inert Gas Stream, Flushing Process, Irradiation Strategy, Positioning, Weld Splashes

Additive Fertigungsprozesse erfreuen sich zunehmender Bedeutung in medialer Berichterstattung, wie auch in der voranschreitenden Forschung. Ein Meilenstein in deren Einsatz wurde durch die Herstellbarkeit direkt einsetzbarer Komponenten, begünstigt durch das vollkommene Aufschmelzen des Rohmaterials in der Prozessführung, erreicht. Auch nach jahrelanger Forschung verbleiben immer noch etliche, weitestgehend unerforschte, sekundäre Einflüsse, deren globaler und zumeist richtungsgebundener Einfluss jedoch nicht unterschätzt werden sollte. Diese Studie beschäftigt sich mit dem flächenbezogenen Oberflächenrauhigkeitsprofil in Abhängigkeit zur Positionierung, welches maßgeblich vom Zusammenspiel des richtungsgebundenen Inertgasstroms und der Belichtungssequenz nachfolgender Einzelquerschnitte, und der damit verbundenen Abfolge in der Entstehung von lokalen Schweißspritzern, mitbestimmt wird. Die Oberflächenrauhigkeit der nach oben gewandten Flächen zeigte enorme Fluktuationen. Die geringsten Rauhigkeiten wurden im zur Maschinenrückwand liegenden Bereich und entlang des Inertgaseinlasses gemessen. Rechtwinklig zur Bauplattform ausgerichtete Flächen wiesen keinerlei Abhängigkeiten zur Inertgasströmung auf. Eine Erhöhung der Belichtungsenergiedichte führte zu einer Verschlechterung der Oberflächenqualität an allen Seitenflächen, jedoch ebenfalls zu einer signifikanten Verbesserung an den nach oben zugewandten Flächen und einer drastischen Reduktion der Schweißspritzer.

Schlüsselwörter: Pulverbettbasierte Additive Fertigung, Inertgasstrom, Flutungsprozess, Belichtungsstrategie, Positionierung, Schweißspritzer

1 Introduction

Selective laser melting belongs to the layer-wise, powder-bed based additive manufacturing technologies and generates components by exposing successive powder layers selectively with a laser beam as the driving force for local solidification [1]. Due to the complete melting of the powder in selective laser melting, this process is capable of manufacturing almost full dense parts within one manufacturing step, proven for stainless steel [2]. The relative density of fabricated components is most

commonly employed as a quality indicator, which has been justified by the relation of the components density to the mechanical properties [3,4] and, specifically for laser beam driven additive manufacturing, the linkage of the relative density to the as-built surface roughness [2,5,6]. Latter dependency is attributed to the coupling of the resulting surface morphology and pore formation on the present melt pool characteristics during manufacture [7,8]. The melt pool itself, on the other hand, depends mainly on the applied energy density of the irradiation,

$$enery\ density = \frac{laser\ power \times exposure\ time}{layer\ thickness \times hatch\ distance \times point\ distance},$$

and the properties of the raw metal powder [9].

In addition to these irradiation dependent factors, there are additional influences based on the inclination angle and the face orientation. The coupling of the layer thickness and the inclination angle of a surface describes the stair size, which is a measure for the shape approximation reasoned in the step-wise generation process [10,11]. Due to the interaction with the neighbouring powder-bed, this staircase effect is superimposed with adjoined and interlaced powder particles, leading to an interconnection of the surface roughness with the powder particle size and the proximate temperature field of the melt pool [12,13].

For many applications the as-built surface quality is insufficient, hence requiring additional steps to overcome this limitation. One option to improve the as-built surface roughness was to extend the manufacturing procedure by including laser re-melting and/or laser erosion [14]. Both approaches were beneficial for the achieved surface roughness; however, the re-melting approach delivered remarkable results coupled with an additional gain in the relative density. Laser erosion, on the other hand, was found to enhance the accuracy of the component and the manufacturability of downwards facing areas without support structure [15]. Nevertheless, both approaches are limited in terms of their accessibility, restricting the modification of most inherent surfaces. To overcome this issue the laser polishing of selective laser melted components was studied, enabling the modification of all surfaces with promising results for further applications [16,17].

To this point, the described surface morphologies were assumed to be homogeneous, however, as shown in a previous study, this is not the case [18].

Emerging weld splashes, arising from the interaction of the laser beam with the powder-bed, influence the surface morphology of every single layer irradiated. Based on the interaction of the inert gas movement with the weld splashes, and their subsequent in-plane appearance, governed by the global irradiation order, a directional pattern arises. Given the importance of the powder layer thickness on the process quality and thus, requiring a homogeneous in-plane powder layer thickness, the inhomogeneities induced by the weld splashes are believed to favour anisotropic in-plane material properties coupled with induced local weak spots [19,20]. Therefore, this study investigated the position dependent surface roughness of fabricated components to identify the in-plane surface roughness distribution.

2 Methodology

2.1 Manufacturing conditions

Samples were fabricated with a SLM 280HL machine (SLM Solutions AG, Lübeck, Germany) equipped with a 400 W ytterbium fibre laser and an available build space of 280 x 280 x 320 mm^3. The utilised irradiation parameters were adapted to the particular region irradiated and two varying sets were considered in this study, *Table 1*. In regard to the necessary support structure, only the block type, i.e. a honeycomb scaffold with open pores and characteristic saw-tooth-like connectors towards the substrate plate and specimens, was applied. The raw 316L (1.4404) stainless steel powder was supplied by SLM Solutions, *Table 2*, *Fig. 1*.

Table 1: Parameter sets utilised
Tabelle 1: Angewandte Belichtungsparameter

Parameter set		Scan speed[1] [mm/s]	Laser power [W]	Hatch distance [mm]	Scan vector length [mm]	Rotation angle increment [°]	Energy density [J/mm³]
(1)	Contour	550	100	0.09	-	-	40.4
	Core	750	175	0.12	7.5	90	38.9
	Final layer	550	175	0.1	-	-	63.6
	Support	650	100	-	-	-	-
(2)	Contour	400	100	0.09	-	-	55.6
	Core	800	200	0.12	10	33	41.7
	Final layer	400	300	0.1	-	-	150.0
	Support	875	200	-	-	-	-
Common		Layer thickness of 50 µm					
		Mounting plate[2] temperature of 200°C					
		Nitrogen is employed as the inert gas					
		Contour is irradiated first, followed by the core, utilising the line scanning strategy					

Table 2: Powder characteristics
Tabelle 2: Pulvereigenschaften

316L (1.4404) powder characteristics	D_{10} [µm]	D_{50} [µm]	D_{90} [µm]	Apparent density [g/cm³]
	22.74	35.54	55.36	3.85

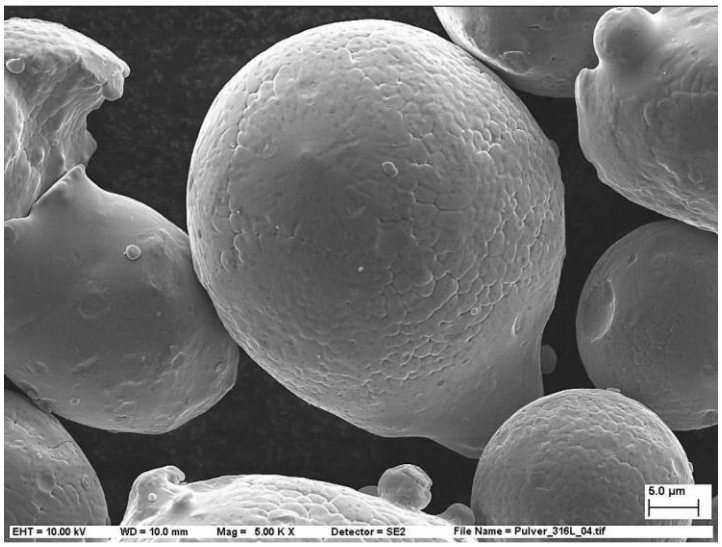

Figure 1: Scanning electron microscope image of the powder particle shape and morphology
Bild 1: Rasterelektronenmikroskopaufnahme, Pulverform und Kornbeschaffenheit

[1] $Scan\ speed = point\ distance\ /\ exposure\ time.$
[2] The substrate plate is fixated on the mounting plate, which includes the thermal regulation.

2.2 Positioning and irradiation sequence

The samples (flat tensile samples DIN 50125 - E 5 x 10 x 40) were built up along their width direction in two distinctive configurations in an almost perpendicular arrangement to each other, *Table 3*. The irradiation sequence chosen starts from the left-door corner and progresses diagonally to the right-back corner, with the y-direction being the primary direction, leading to a particular irradiation pattern, *Fig. 2, 3*. Hence, the irradiation sequence is in reversed direction to the inert gas stream, which flows in positive y-direction. This particular coupling generally ensures that there are no interactions of the deposited powder layer with the emerging weld splashes of the ongoing process. Thus, the loose powder remains undisrupted prior to irradiation, but to the cost of the interaction of the weld splashes with the solidified areas.

Table 3: Orientation in dependency to the longitudinal axis of the specimen
Tabelle 3: Platzierung in Abhängigkeit zu der Probenlängsachse

Configuration	α_{XY}	α_{X}
(a)	0°	5°
(b)	0°	85°

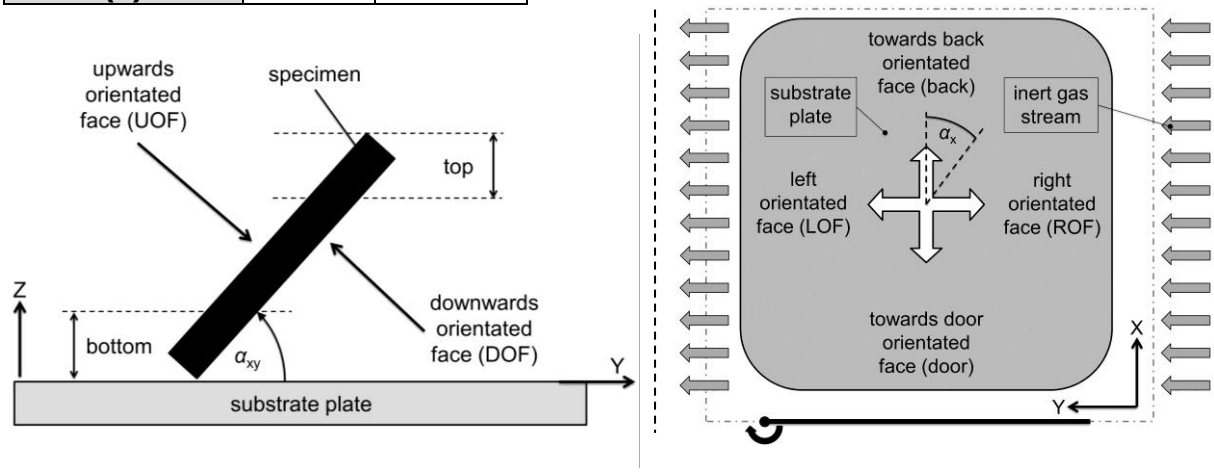

Figure 2: Applied nomenclature for description of surface orientations, adopted from [18]
Bild 2: Angewandte Nomenklatur für Oberflächenorientierungen, übernommen von [18]

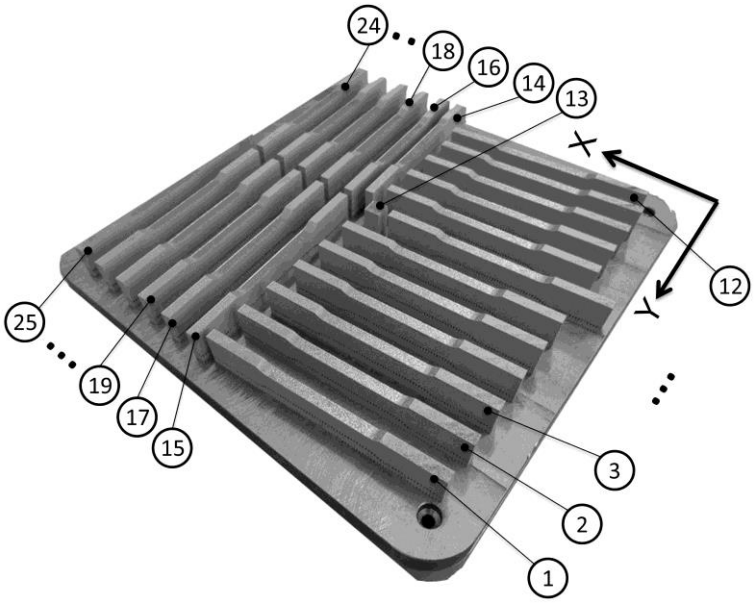

Figure 3: Positioning of samples and sequence of irradiation[3]
Bild 3: Positionierung der Proben und Belichtungsabfolge[3]

2.3 Surface quality

Surface quality measurements were conducted in accordance with the ISO 25178 standard with an optical Zemetrics Zegage white light interferometer (Zygo Corp., Middlefield, CT, USA). Three area increments (800 x 800 µm^2) were evaluated along the length axis on the UOF and side faces (i.e. LOF, ROF, back, door) of each sample, based on which Ra and Rz values were determined. It should be mentioned that the edge effect, influencing the UOF's, was not considered within the measurements; the values given solely reflect the stable surface morphology in adequate distance to the borderlines [21]. Given the very limited height difference of the inherent UOF's along the samples under consideration, the results were projected into an averaged 2D representation and interpolated along the xy-plane.

3 Results and discussion

Two distinctive surface morphologies were evident based on the alignment, *Fig. 4*: The surface roughness of vertically aligned side faces was governed by the interaction with the loose neighbouring powder particles, whereas the UOF's were governed by the scan track pattern of the final layer superimposed with scattered weld splashes. No influences of the surface roughness of the side faces to the inert gas stream were evident. The ROF's and LOF's, which respectively were facing or

[3] Irradiation number ⑬ refers to a cubic sample placed in the centre.

averting the inert gas stream, did not reveal any noteworthy deviations, *Fig. 5*. Minor discrepancies were present between the back and door facing surfaces, whereby the door surfaces continuously revealed lower roughness values. Given the two-way recoating procedure applied during manufacturing, the reason for this is, to date, not precisely clarified.

The comparison of the results between the two parameter sets revealed significant variations in the surface roughness. In general, the parameter set (2) applied a higher energy density throughout all areas, which led to a noticeable overall increase in roughness on all side faces, attributed to the increased interaction of the surrounding powder particles with the heat affected zone, but to a remarkable roughness reduction of the UOF's, Table 1. Moreover, the scatter in surface roughness of the UOF's, mainly caused by the weld splashes, was significantly decreased. The latter has been investigated further by creating interpolated surface roughness maps for the xy-plane based on the results of the UOF's, *Fig. 6*. Both parameter sets showed tendencies of an increase in surface roughness along the positive y-direction, however, far more pronounced in the case of parameter set (1). A constant area of increased surface roughness was revealed in the door area (x = 0-80 mm), apart from the region close to the right. In addition, a clear trace of weld splashes was evident in the centre region (x ~140 mm), starting at the third configuration (a) sample counted from the right, lancing to the left border, irradiation number ⑩ in Fig. 3. In general, the following holds for the in plane surface roughness of UOF's, if diagonally divided in two sections, the triangle along the right-back boundaries exhibited, in both cases, fairly constant and comparably low surface roughness results. Towards the left border, the likelihood of weld splashes, and correspondingly the measured surface roughness, increased. The cause of the increased surface roughness along the door boundary is not identified yet. However, it is believed that this phenomenon is linked with the compensation of the focus offset and change in the incidence angle of the laser beam.

Based on the high dependency on the chosen irradiation parameters and their variation according to the utilised raw material, it can be anticipated that both the surface roughness and the emphasis on the in plane pattern fluctuate. This relation

restricts global predictions for the surface roughness to directional dependencies, as the absolute magnitudes underlie various influences and alterations.

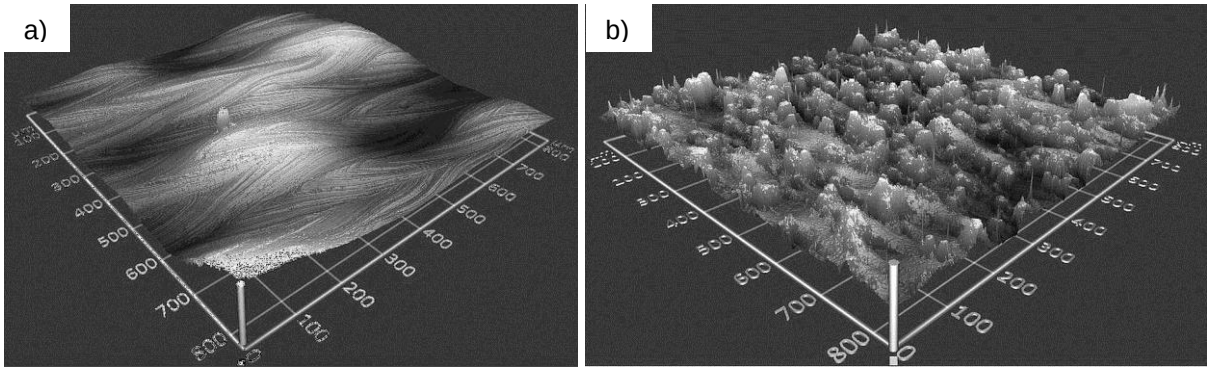

Figure 4: Surface morphology of a) vertically aligned side faces and b) horizontally aligned UOF‘s
Bild 4: Oberflächenbeschaffenheit der a) vertikal ausgerichteten Seitenflächen und b) horizontal ausgerichteten Deckflächen (UOF‘s)

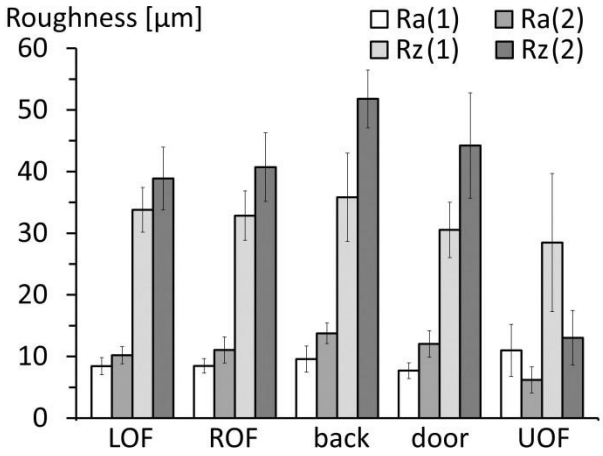

Figure 5: Surface roughness and standard deviation per configuration and face alignment
Bild 5: Oberflächenrauhigkeit und Standartabweichung pro Konfiguration und Ausrichtung der Oberfläche

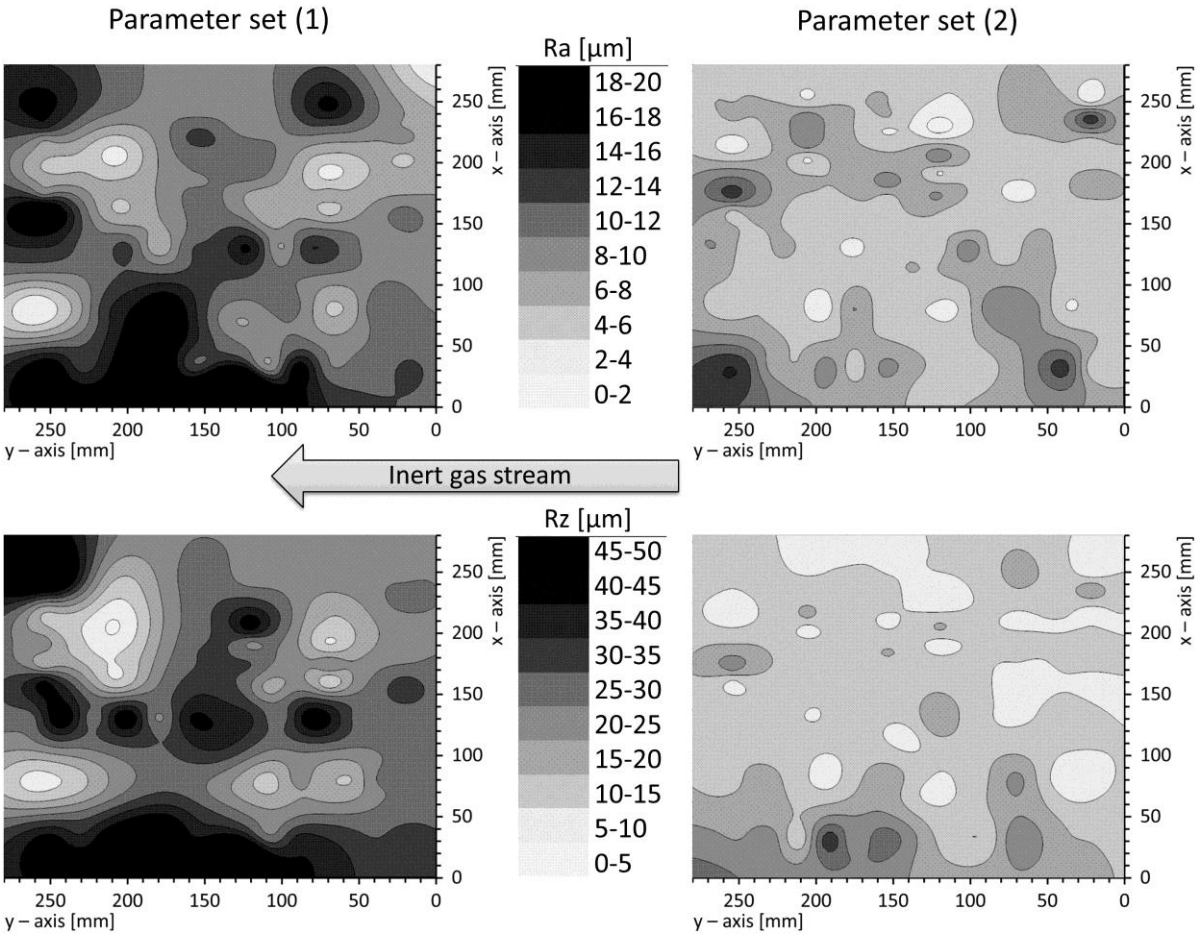

Figure 6: Dependency of the surface roughness of UOF's on the positioning on the substrate plate and the irradiation parameters
Bild 6: Abhängigkeit der Oberflächenrauhigkeit der Deckflächen (UOF's) von der Positionierung auf der Bauplattform und der Belichtungsparameter

3.1 Overview of documented surface roughness

In order to categorise and frame the surface roughness values of this study in the big picture, an overview, representing results documented in related investigations, is provided, *Table 4*. It needs to be noted that the various research groups have utilised varying equipment and processing settings; thus, results are often not directly comparable.

Table 4: Surface roughness results documented in literature; given values refer to as-built surfaces
Tabelle 4: Ergebnisse für die Oberflächenrauhigkeit aus Literaturquellen; alle Angaben beziehen sich auf unbehandelte Oberflächen

	Ra [µm]	Rz [µm]	Material	Surface orientations covered
Cherry et al. [2]	9-16	-	316L	side faces, 90° to substrate plate (LOF, ROF, door, back)
Kempen et al. [22]	14.7 - 18.3	-	HSS M2	UOF (T_{Base} = 90°C; 200°C)
Kruth et al. [14]	7.2 – 18.8	-	316L	UOF
Löber et al. [12]	15.03	23.04	316L	side faces, 90° to substrate plate (LOF, ROF, door, back)
Spierings et al. [9]	5-10	-	316L	UOF
Strano et al. [13]	9.2 – 16.1	-	316L	surface inclinations 0° - 90° to substrate plate in 5° intervals
Yasa et al. [15]	16 – 28	-	316L	UOF with 10° and 30° inclination
Yasa et al. [23]	15	-	316L	UOF
SLM Solutions [24]	10 ± 2	50 ± 12	316L	-
This work	6.20 – 13.76	13.04 – 51.79	316L	LOF, ROF, UOF, door, back surface inclinations 0°, 90°
Previous work [18]	5.75 – 27.02	13.88 – 158.19	AlSi10Mg	LOF, ROF, UOF, DOF, door, back surface inclinations 0°, 45°, 90°

3.2 Warping

Apart from the surface roughness, the samples, already at their relatively low build height of 15 mm, revealed a recognisable warping along their width direction, *Fig. 7*. These deformations perpendicular to the build direction were evident for both configurations and parameter sets and resulted from the internal residual stresses exceeding the yield strength, leading to plastic deformations during the manufacturing process [25].

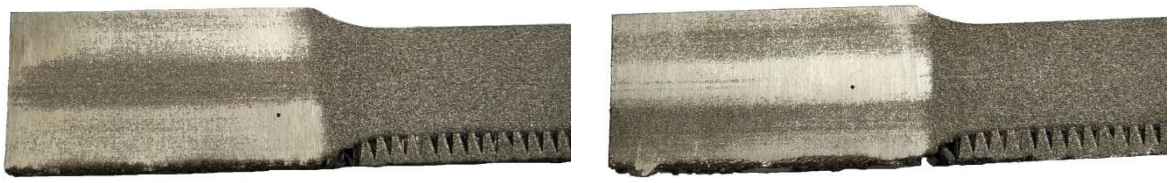

Figure 7: Geometric deviations perpendicular to build direction occurred due to thermal induced stresses
Bild 7: Geometrische Abweichungen senkrecht zur Baurichtung aufgrund thermisch induzierter Spannungen

4 Conclusion

Samples built with two parameter sets revealed major dependencies of their surface roughness on the applied irradiation energy density and for the UOF's, considerable fluctuations in the xy-plane. Faces perpendicular to the substrate plate, showed no interconnection with the irradiation sequence and inert gas stream, but a remarkable volatility to the irradiation settings. In particular, an increased energy density led to an increased surface roughness throughout all side faces. Contrary to this, the roughness of UOF's improved with an increased irradiation energy density and the appearance of adjoined weld splashes on the solidified areas drastically decreased. In general, the following could be concluded for the in plane surface roughness tendencies of UOF's: the best results were achieved in the area close to the inert gas inlet and towards the back, whereas the areas in close proximity to the door and the inert gas outlet revealed a drastic increase in surface roughness.

5 Acknowledgement

Sincere appreciation to Michael Sedlmajer and Rene Klink for their helpful support throughout the implementation and evaluation of the experiments.

6 References

[1] I. Gibson, D. W. Rosen, B. Stucker, Additive Manufacturing Technologies, Springer-Verlag US, New York, USA **2010.**
[2] J. A. Cherry, H. M. Davies, S. Mehmood, N. P. Lavery, S. G. R. Brown, J. Sienz, *Int. J. Adv. Manuf. Technol.* **2015**, *76*, 869.
[3] S. Kleszczynski, J. zur Jacobsmühlen, J. Sehrt, G. Witt, Digital Product and Process Development Systems: Mechanical Properties of Laser Beam Melting Components Depending on Various Process Errors, Springer Berlin Heidelberg, **2013.**
[4] A. Öchsner, Continuum Damage and Fracture Mechanics, Springer, Singapur **2016.**

[5] G. Casalino, S. L. Campanelli, N. Contuzzi, A. D. Ludovico, *Opt. Lasers Technol.* **2015**, *65*, 151.
[6] C. Qiu, C. Panwisawas, M. Ward, H. C. Basoalto, J. W. Brooks, M. M. Attallah, *Acta Mater.* **2015**, *96*, 72.
[7] D. Dai, D. Gu, *Int. J. Mach. Tools Manuf.* **2015**, *88*, 95.
[8] N. T. Aboulkhair, N. M. Everitt, I. Ashcroft, C. Tuck, *Addit. Manuf.* **2014**, *1-4*, 77.
[9] A. B. Spierings, N. Herres, G. Levy, *Rapid Prototyping J.* **2011**, *17*, 195.
[10] B. Vandenbroucke, J. P. Kruth, *Rapid Prototyping J.* **2007**, *13*, 196.
[11] J. P. Kruth, B. Vandenbroucke, J. Van Vaerenbergh, I. Naert, *J. Dent. Technol.* **2007**, 24.
[12] L. Löber, C. Flache, R. Petters, U. Kühn, J. Eckert, *Rapid Prototyping J.* **2013**, *19*, 173.
[13] G. Strano, L. Hao, R. M. Everson, K. E. Evans, *J. Mater. Process. Technol.* **2013**, *213*, 589.
[14] J. P. Kruth, E. Yasa, J. Deckers, Roughness Improvement in Selective Laser Melting University of Leuven. https://lirias.kuleuven.be/bitstream/123456789/197936/2/08pp075.doc. accessed 28/04/2016.
[15] E. Yasa, J. P. Kruth, J. Deckers, *CIRP Ann. Manuf. Techn.* **2011**, *60*, 263.
[16] J. Schanz, M. Hofele, L. Hitzler, M. Merkel, H. Riegel, Machining, Joining and Modifications of Advanced Materials: Laser polishing of additive manufactured AlSi10Mg parts with an oscillating laser beam, Springer, Singapore **2016.**
[17] J. Schanz, M. Hofele, S. Ruck, T. Schubert, L. Hitzler, G. Schneider, M. Merkel, H. Riegel, Mat.-wiss. u. Werkstofftech. 2017, 48, 463.
[18] L. Hitzler, C. Janousch, J. Schanz, M. Merkel, F. Mack, A. Öchsner, *Mat.-wiss. u. Werkstofftech.* **2016**, *47*, 564.
[19] K. Abd-Elghany, D. L. Bourell, *Rapid Prototyping J.* **2012**, *18*, 420.
[20] L. Hitzler, C. Janousch, J. Schanz, M. Merkel, B. Heine, F. Mack, W. Hall, A. Öchsner, *J. Mater. Process. Technol.* **2017**, *242*, 48.
[21] E. Yasa, J. Deckers, T. Craeghs, M. Badrossamay, J. P. Kruth, *SFF Symposium* **2009**, 180.
[22] K. Kempen, B. Vrancken, S. Buls, L. Thijs, J. Van Humbeeck, J.-P. Kruth, *J. Manuf. Sci. Eng.* **2014**, *136*, 061026.
[23] E. Yasa, J. Deckers, J.-P. Kruth, *Rapid Prototyping J.* **2011**, *17*, 312.
[24] SLM Solutions, SLM-Metal-Powder. http://stage.slm-solutions.com/index.php?downloads_en. accessed 16/03/2016.
[25] J. P. Kruth, J. Deckers, E. Yasa, R. Wauthle, *P. I. Mech. Eng. B-J. Eng.* **2012**, *226*, 980.